Optik - International Journal for Light and Electron Optics 231 (2021) 166282

Contents lists available at ScienceDirect

Optik

journal homepage: www.elsevier.com/locate/ijleo

Original research article

Optical performance of aluminum mirror for cryogenic applications

Fuhe Liu [a,b,*], Ping Jia [a,b], Honghai Shen [a,b], Yongsen Xu [a,b]

[a] Changchun Institute of Optics, Fine Mechanics and Physics, Chinese Academy of Sciences, Southeast Lake Road, Changchun, China
[b] University of Chinese Academy of Sciences, Shijingshan District, Beijing, China

ARTICLE INFO

Keywords:
Collimator
Aluminum mirror
Cryogenic deformation
Surface figure measurements

ABSTRACT

Aluminum mirrors are most commonly used for cryogenic optic systems. A parameter simulation has been conducted to design the aluminum mirror. We have obtained an optimized mirror structure after optimization applied in the mirror design stage. A finite element model analysis was conducted to predict the gravity sag, mounting-induced error and cryo-deformation of the mirror. Then we have fabricated a 160 mm diameter aluminum mirror based on the optimization results, tested it at room and cryogenic temperature. An error budget developed based on the experimental results shows that the fastening preloads effect dominates the surface figure of the aluminum mirror. The total deformation of the mirror surface at 100 K meets the optical requirement, which indicates that the optimized aluminum mirror is stable enough to retain good surface figure at cryogenic temperature and the aluminum mirror is promising for its cryogenic applications.

1. Introduction

Good thermal stability and high thermal conductivity are major advantages of aluminum material, which makes aluminum mirrors most commonly used for cryogenic optic systems. Furthermore, aluminum mirrors are relatively low cost as long as they can be diamond point machined and post polished. Therefore, we choose aluminum as the mirror material for the cryogenic collimator, a Chinese infrared simulation facility. The collimator will be cooled to 100 K in a vacuum chamber by a liquid nitrogen cooling device. Aluminum mirrors used in cryogenic environment have brought about challenges, such as mirror structure design, heat treatments, bimetallic bending and conductive heat transfer [1–5].

This article focuses on research into the structure design and cryogenic optical testing of the aluminum mirror. The mirror structure directly affects the surface profile, so that it is important to ensure that the mirrors retain static and thermal stable when operated in the cryogenic environment, which is the key to meeting the requirements of the collimator.

So far, aluminum mirrors with outboard mounting flanges with three raised pads have been mainly adopted in the infrared instruments. For example, the cryogenic mirrors of the Alignment Monitor System telescope and the K-mirror assembly for NIRSPEC employed the outboard mounting flanges structure. With the aperture of the mirror becoming larger, starting at about 150−250 mm, outboard mounting flanges become less practical and back mounted approaches are more commonly used. The aspheric and flat mirrors of the PORTS are back mounted as long as the mirrors are more than 200 mm in diameter [6]. Considering the mirror size of

* Corresponding author at: Changchun Institute of Optics, Fine Mechanics and Physics, Chinese Academy of Sciences, Southeast Lake Road, Changchun, China.
E-mail address: liusong0804@126.com (F. Liu).

https://doi.org/10.1016/j.ijleo.2021.166282
Received 10 September 2018; Accepted 7 January 2021
Available online 5 February 2021
0030-4026/

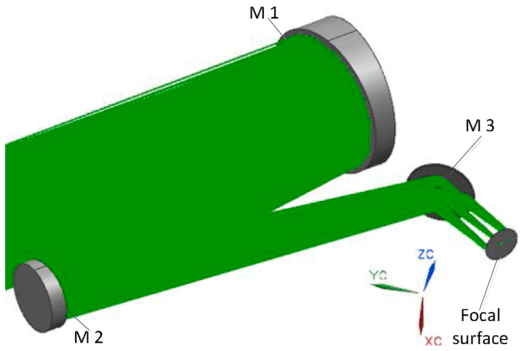

Fig. 1. A schematic view of the optical system for the collimator.

Table 1
Optical Requirements of the mirrors.

Mirror	M1	M2	M3
RMS(nm)	63	63	63

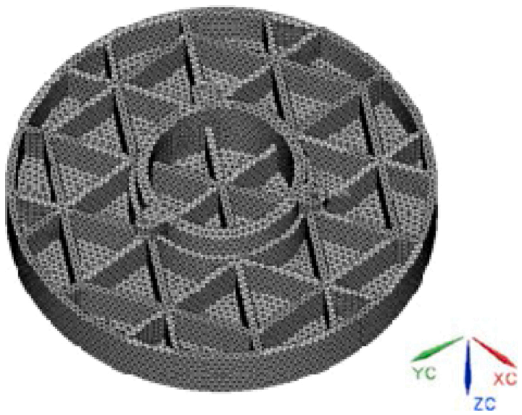

Fig. 2. Finite element models of M3.

the collimator researched in this article, a back mounted approach is adopted as the mirror structure.

Cryogenic collimators usually experience a large temperature change from the ambient to the cryogenic environment. The stiffness and strength of the mirror can directly guarantee the optical performance at cryogenic temperature. Therefore, many researchers have done plenty of work on the mirror structure design for cryogenic instruments. For example, Daniel Vukobratovich et al. developed a mirror structure for the Gemini Near Infrared Spectrograph and studied the heat treatment process to minimize residual stress in the mirror [7]. Moon et al. have designed different types of aluminum mirrors and studied the optical performance caused by bimetallic under cryogenic environment [8]. Shen from China has designed and tested the aluminum mirror at 100 K for a cryogenic Richey-Chretien system [9].

To improve present research, we have conducted an optimization on the model of the mirror developed in this paper. In this way, we have obtained a mirror structure with high stiffness and thermal stability for the collimator. We have fabricated a 160 mm diameter aluminum mirror based on the optimization results, and tested it at room and cryogenic temperature. Finite element analysis and experimental results indicate that the mirror structure presented in this paper has met the requirements of the cryogenic collimator under development.

2. Mirror structure design

As seen in Fig. 1, the off-axis optical system of the collimator has three mirrors, both the primary mirror and the second mirror are hyperbola, the third mirror is flat and is used to reduce the length of the whole system. We haven't used the aluminum mirror before, so we started the research with the flat mirror, M3 in this paper. In particular, the M3 studied in this paper is 160 mm in aperture. The collimator has requirements for its total wave front to be no more than 218 nm rms at100 K, which indicates that the surface figure of

Table 2
Material Properties of RSA-6061.

Density(kg/m^3)	Elastic Modulus(MPa)	Poisson Ratio
2700	7000	0.33

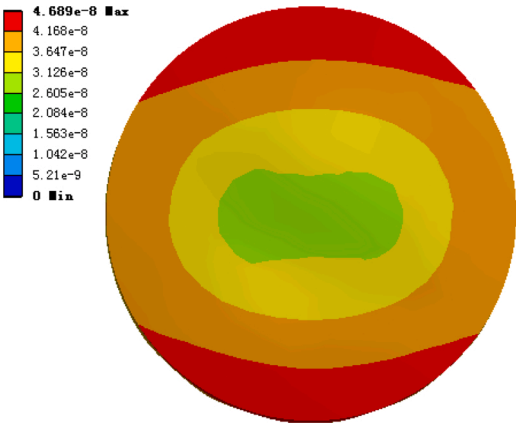

Fig. 3. Total deformation of optimized mirror.

M3 must be less than 63 nm rms at 100 K. The optical requirements for all the components are listed in Table 1.

According to the optical system presented in Fig. 1, the finite element model of M3 was established, as show in Fig. 2. The mirror design is an open back, light weighted design with a rear integral mount flange. The design of the mount flange is to increase the stress transfer length to the mirror surface, which reduces the mount induced deformation to the mirror surface [10]. The mirror is tightened to the optic bench by 3 bolts on the flange. Compared to the conventional AA-6061, RAS-6061 T6 aluminum is selected as the mirror material as long as its advantage of outstanding surface finish. The properties of the RAS-6061 T6 aluminum are listed in Table 2.

Parameter analysis of the mirror based on goal driven optimization was applied in this paper using the finite element model software Workbench.

The optimization model is given as follows:

Optimization objective:

$$\text{Minimize} C_x \tag{1}$$

Constraints:

$$3\ \text{mm} \le t_1 \le 8\ \text{mm} \tag{2}$$

$$2\ \text{mm} \le t_2 \le 6\ \text{mm} \tag{3}$$

$$10\ \text{mm} \le h \le 20\ \text{mm} \tag{4}$$

$$m \le 0.8\ \text{kg} \tag{5}$$

Design variable:

t_1, t_2, h

where C_x is the objective function, C_x is the maximum displacement of the whole mirror under gravity in the X direction. t_1 is the thickness of the mirror surface, t_2 is the thickness of the back side ribs, h is the height of the back side ribs. M is the mass of the finite element model, the upper bond of which is 0.8 kg. The initial value for t_1, t_2 and h are 5 mm, 3 mm and 15 mm.

The boundary conditions and constraints for the finite element model are shown as below:

1 The mirror was placed with the optical axis horizontal.
2 Fix the fitting surface of the mount flange.
3 The orientation of gravity coincides with the X. axis.
4 The material properties of the finite element model are listed in Table 2.

The simulation results show that the optimized mirror has a 5 mm thickness for the surface, 4 mm thickness and 15 mm height for the back side ribs; the total mass of the optimized mirror is 0.61 kg. According to the deformation cloud image of the optimized mirror

Table 3
Fastener pressures on the mirror.

Ts (Nm)	0.6	0.7	0.8	0.9	1.0
F(nm)	1052	1228	1403	1579	1754

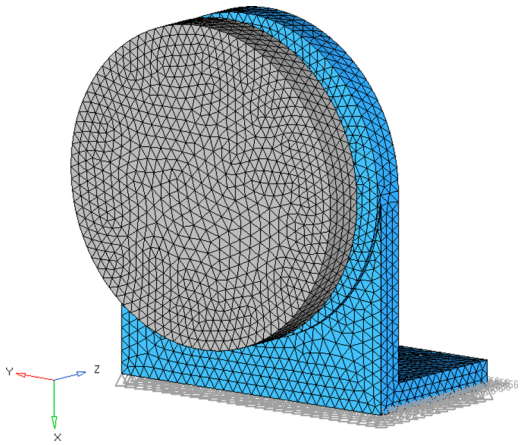

Fig. 4. Finite element models of the mirror assembly.

Table 4
Mirror surface figure under fastening preloads.

Preload(N)	1052	1228	1403	1579	1754
RMS(nm)	32.8	35.1	37.2	39.6	41.9

shown in Fig. 3, the maximum displacement of the mirror under a gravity load in the X direction is 46.8 nm. The lightweight result that is obtained by the goal driven optimization can be used directly in practical applications. Therefore, the mirror structure was designed based on the optimization results.

3. Finite element analysis

In order to prove the possibility of the optimization design method for the mirror, a finite element model analysis of the mirror was carried out.

The mirror is easy to deform under external pressure due a low Young's modulus of the mirror material aluminum. Only if the mirror surface figure meets the requirements listed in Table 1, will the collimator operate satisfactorily at cryogenic temperature. As a result of that, the mirror structure with high static and thermal stability, must overcome the influence induced by gravity, mounting loads and cryogenic temperature.

In the assembly design of the mirror, the mirror was fastened to the optical bench by 3 bolts. Torque is used to control the bolt preload, which can be expressed as follows [11]:

$$F = \frac{T_s}{u_s d_1 \sec\beta + P/2\pi} \tag{6}$$

where T_s is the torque applied to the fastener (this analysis selects 0.6 N m 0.7 N m 0.8 N m 0.9 N m and 1.0 N m for T_s), F is the fastener pressure on the mirror, d_1 is the diameter of the bolt (this paper selects 4 mm for d_1), P is the pitch of the threads (this paper selects 0.7 mm for P), u_s is the friction coefficient between the threads(this paper selects 0.1 mm for u_s), and β is the half-angle of the threads(this paper selects 30° for β). Table 3 shows the fasten pressure on the mirror calculated from the equation.

As shown in Fig. 4, the finite element model of the mirror assembly was developed based on the optimization results. The model consists of the mirror and one optical bench, the boundary conditions and constrains are given as follows:

1 Fix the bottom of the optical bench.
2 The mirror was connected with the optical bench by use of a rigid connection, REB2.
3 The material properties of the mirror and the bench in Fig. 4 are shown in Table 2.

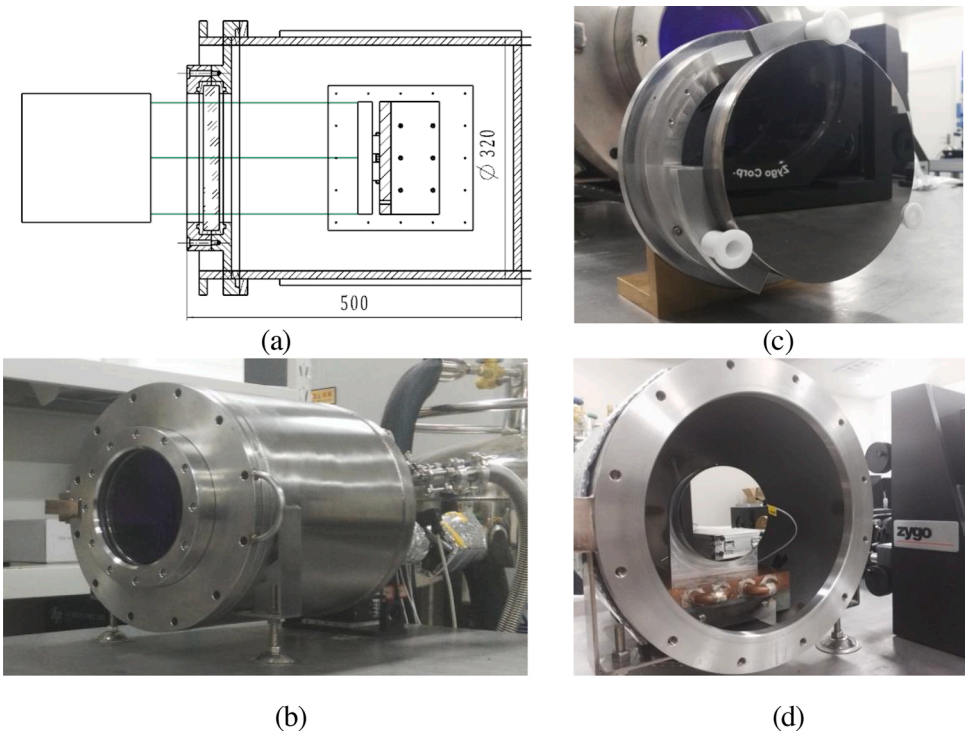

Fig. 5. (a) Test setup of the mirror. (b) Liquid-nitrogen cooled chamber that was used for optical measurement of the mirror. (c) Aluminum mirror supported by the contrastive supporting structure. (d) Aluminum mirror mounted to the bench with the rear flange.

4 Seven load cases were applied to the finite element model: gravity in the X-axis at room temperature, gravity in the X-axis at 100 K and five load cases with preloads from Table 4 at room temperature.

The initial position and the displacement of nodes on the mirror surface were exported to Matlab after the finite element analysis. After the post processing of the surface data, the analysis results show that the mirror surface figure is 5.2 nm rms under gravity at room temperature and 7.3 nm rms at 100 K. According to the analysis results, the effect caused by the gravity is very small, which shows that the mirror is stiff enough to remain a good surface figure under gravity. The analysis results indicate that the mirror has very similar surface figure from room temperature to 100 K. This is because the mirror and the bench are designed from the same material of aluminum 6061 that the temperature fluctuation will bring about a relatively small effect.

The surface figures of the mirror caused by the fastening preloads are listed in Table 4. The results show that the deformation of the mirror increases with the growing of the bolt preloads, which means the researchers and the engineers could choose the appropriate fastening preloads to make the mirror surface figure meet the optical requirements.

4. Experimental verification and results

According to the optimization results, we have fabricated a 160 mm diameter aluminum mirror and have done a deep investigation on the performance of mirror surface figure. In contrast to the nickel plated mirrors, bare-polished mirrors eliminate the surface figure error induced by the bi-metal interfaces over a large reduction in temperature [12–14]. In this paper, the mirror was rough figured utilizing conventional machining, the rear fitting surface of the mirror was fine machined with the flatness less than 2 μm. Then the mirror surface was diamond point machined and bare polished. Different types of experiments were planned and then completed on the mirror.

4.1. Surface figure under gravity

In order to evaluate the surface figure of the aluminum mirror under gravity, a contrastive supporting structure was designed and fabricated, as is shown in Fig. 5(c). In the horizontal direction, two cylinder rods sustain the mirror. A clip is applied at the top of the mirror to avoid tilting forward. The design of the supporting structure in Fig. 5(c) eliminates the mirror surface figure error caused by the mount bending under gravity. Furthermore, in another experiment, as is shown in Fig. 5(d), the mirror was mounted to the bench through its rear mount flange with 3 bolts. The preloads of the bolts are extremely small, which makes the mirror nearly hung on the bolts. In this way, the deformation induced by the fastening preload can be ignored. The only factor that affects the mirror surface figure was the bending of the mount under the weight of the mirror.

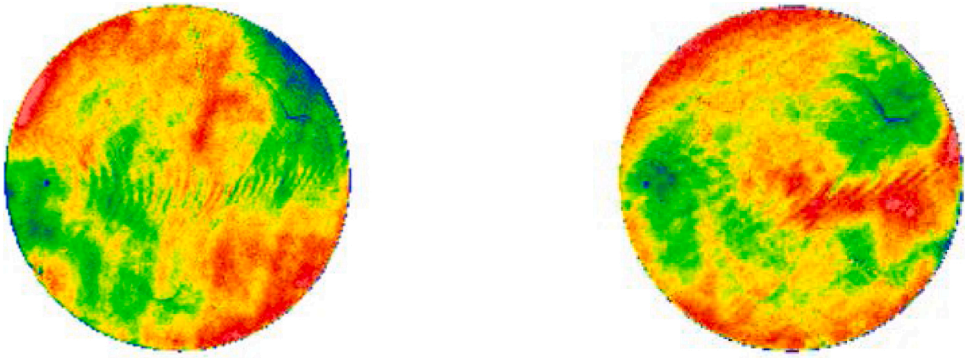

Fig. 6. (a) Mirror surface figures after fabrication. (b) Mirror surface figures under gravity.

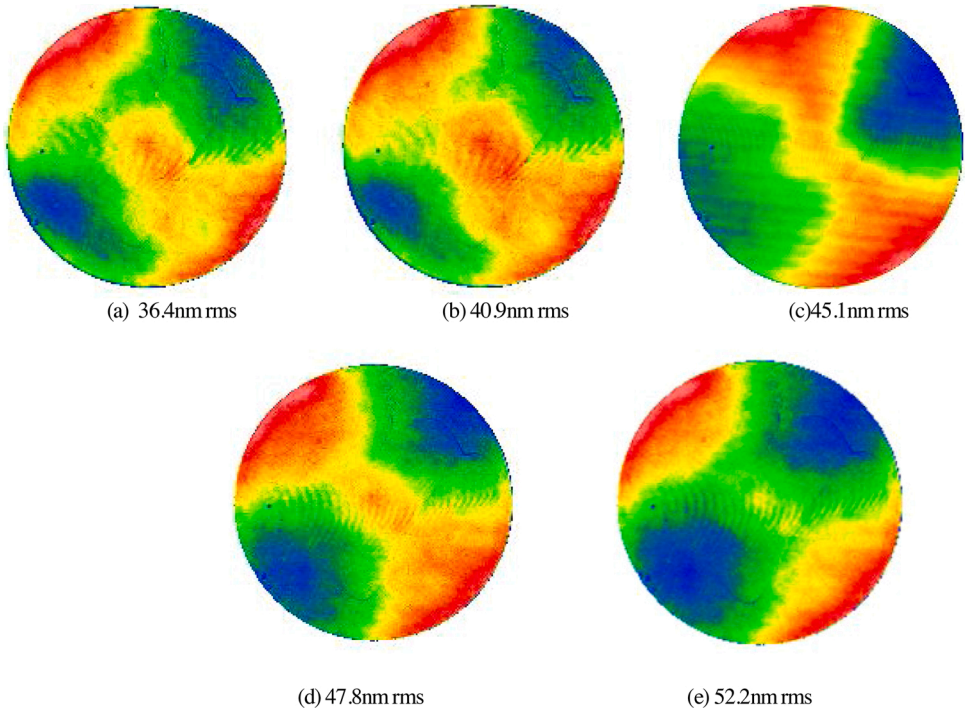

Fig. 7. Surface figures of the aluminum mirror after subtraction of the figure in Fig.6 (b) with fastening preloads (a) 0.6 N m, (b) 0.7 N m (c) 0.8 N m, (d) 0.9 N m, (e) 1.0 N m.

The mirror surface figure was measured by the ZYGO interferometer. According to the surface figures in Fig. 6, the contrastive supporting structure and back mounted assemblies show very similar results. The gravity induced error was 6.4 nm rms after the figure of Fig. 6(a) was subtracted from Fig. 6(b). The finite element model analysis of the mirror surface figure shows a good agreement with the measurement. The experiments show that the 6061 mirror is stable enough to result in minimal surface figure when the flange mount sustains the weight of the mirror.

4.2. Surface figure under fastening preloads

The surface strain caused by the fastening preloads can damage the surface figure badly, which will make the mirror deformation unacceptably large for the collimator. In order to reduce the mount induced deformation to the mirror surface, a back mount flange is designed to increase the stress transfer length to the mirror surface. As is seen in Fig. 5(d), fastening preloads with varying values are applied on the bolts of the mirror, then the mirror surface figure results corresponding to different preloads were measured by the interferometer.

In Fig. 7(a)–(e), the mirror surface figures are presented after subtraction of the initial surface figure in Fig. 6(b). The results

Table 5
RMS of the Zerodur Mirror.

Mirror conditions	Room temperature	100 K
With K9 window	16.8 nm	17.3 nm

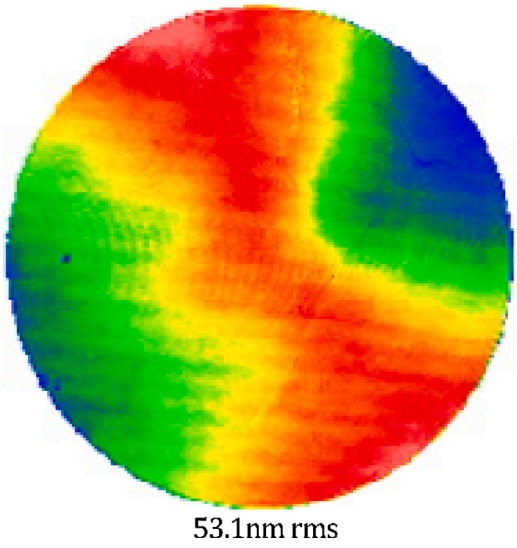

Fig. 8. Total surface figure of the mirror at 100 K.

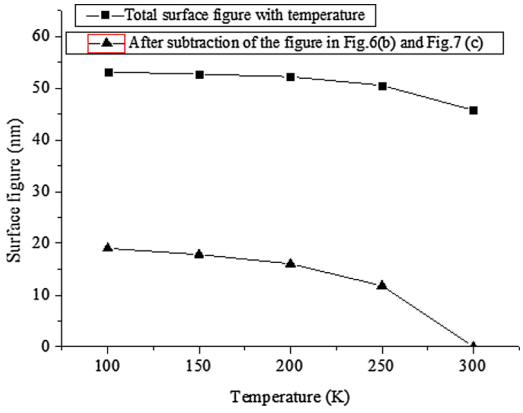

Fig. 9. Total mirror surface figure with temperature and change of the mirror surface figure after subtraction of the surface figure in Figs. 6(b) and 7 (c).

indicate that the fastening preloads have a big influence on the mirror surface figure. The results also show larger astigmatism of the mirror surface with the growing of the mounting preloads. The experimental results are about 30% bigger than the finite element model analysis, due to the impact of flatness of the components. The optical performance could be improved by reducing flatness of the fitting surface.

4.3. Surface figure at cryogenic temperature

Before the cryogenic optical test for the aluminum mirror, an experiment with a zerodur mirror was conducted to verify the influence induced by the K9 window [15,16]. The surface figures of the zerodur mirror with window, from room temperature to 100 K, have been measured before the test mirror. Thanks to the good thermal isolation of the MLI, the temperature of K9 window maintained around 293 K during the test. The test results are given in Table 5.

The measured data in Table 5 were exported to the software, the simulation results showed that the wave front error of the K9 window was less than 6 nm rms, which gave a small influence on the measured mirror. The data listed in the cryogenic test below are

Table 6
Error budget of the mirror surface figures.

Total surface figure	53.1 nm
Fabrication error	16.5nm
Gravity sag	7.1 nm
Mount-induced error	45.1 nm
Cryo-deformation	19.2 nm

corrected for the effect of the K9 window.

Then we placed the mirror in the vacuum chamber shown in Fig. 5(b) and measured the optical performance of the mirror at cryogenic temperature. The fastening preloads of the three bolts were set to 0.8 N m in the following tests. As is shown in Fig. 5(a), there is a Zygo interferometer in front of the chamber. A three-axis adjustment support is placed on the bottom of the chamber. The inner atmosphere of the chamber was less than 0.1 Pa with the help of the vacuum pump. The mirror was conductively cooled by the cold plate. Two thermometers were attached to the mirror; one was at the back ribs, and the other was on the edge of mirror. Except for the beginning cooling stage, the difference in temperature between the two thermometers was less than 3 K, indicating a fine thermal conductivity of the aluminum material even at cryogenic temperature. The mirror surface figures were measured at different temperatures while the mirror was being cooled down.

The total surface figure of the mirror at 100 K is presented in Fig. 8. Fig. 9 shows two graphs, one is the change of the total mirror surface figure with the temperature, and the other is the change of the mirror surface figure caused by the temperature shown after subtraction of the surface figure Figs. 6(b) and 7 (c). The change in cryogenic deformation of the mirror is 19.2 nm rms at 100 K, more than two times the figure of the analysis results. This is likely because the residual stress in the mirror affected the surface when the mirror was being cooling down. An error budget was developed based on the experiments in Table 6. The fastening preloads effect dominates the surface figure of the aluminum mirror. According to the deformation of the mirror shown in Table 6, the total surface figure of the mirror at 100 K is 53.1 nm rms. The optimized mirror meets the optical requirements in Table 1 at cryogenic temperature. Hence the optimized mirror is promising for its application to the cryogenic collimator.

5. Conclusion

This paper introduces an optimization design, a finite element model analysis, and optical performance tests of an aluminum mirror for a cryogenic collimator. An optimized mirror structure was obtained after the parameter optimization applied in the mirror design stage. A finite element model analysis was conducted to predict the gravity sag, mounting error and cryo-deformation of the flat mirror. Then we have fabricated a 160 mm diameter aluminum mirror based on the optimization results, tested it at room and cryogenic temperature. An error budget developed based on the experiments results shows that the fastening preloads effect dominates the surface figure of the aluminum mirror. The total deformation of the mirror surface at 100 K meets the optical requirement, which indicates that the optimized aluminum mirror is stable enough to retain good surface figure at cryogenic temperature and the aluminum mirror is promising for its cryogenic applications.

Acknowledgements

The authors would like to thank Dr. Zhang for his work in the mirror machining and polishing.

References

[1] Jason E. Hylan, Leroy M. Sparr, Raymond G. Ohl, John Eric Mentzell, Matthew A. Greenhouse, John W. MacKenty, Lessons learned from the design, fabrication, integration, and test of a cryogenic, IR spectrometer for ground-based astronomy, Proc. SPIE 5172 (2003) 48–59.
[2] Daniel Vukobratovich, J.P. Schaefer, Large stable aluminum optics for aerospace applications, Proc. SPIE 8125 (2011) 81250T.
[3] Vania Da Deppo, Kevin Middleton, Mauro Focardi, Gianluca Morgante, Emanuele Pace, et al., Design of an afocal telescope for the ARIEL mission, Proc. SPIE 9904 (2016) 990434.
[4] T. Newswander, B. Crowther, G. Gubbels, R. Senden, Aluminum alloy AA-6061 and RSA-6061 heat treatment for large mirror applications, Proc. SPIE 8837 (2013) 883704.
[5] Michael Sweeney, Design and manufacturing technologies for all-reflective collimators, relays, and derotating assemblies in cryovac instruments, Proc. SPIE 4822 (2002) 1–11.
[6] Michael Sweeney, Robert Spinazzola, Donald Morrison, Dennis Macklin, Jared Marion, Advanced manufacturing technologies for reduced cost and weight in portable ruggedized VIS-IR and multi-mode optical systems for land, sea, and air, Proc. SPIE 8012 (2011) 801227.
[7] Daniel Vukobratovich, Ken Don, Richard Sumner, Improved cryogenic aluminum mirrors, Proc. SPIE 3435 (1998) 9–18.
[8] I.K. Moon, M.K. Cho, R.M. Richard, Optical performance of bimetallic mirrors under thermal environment, Proc. SPIE 4444 (2001) 29–40.
[9] Shen Mangzuo, Wenli Ma, Sheng Liao, Xiaohong Zhang, Development of a cryogenic optical system, Acta Opt. Sin. 21 (2001) 202–205.
[10] G. Mondello, A. Novi, C. Devilliers, Development of sintered-SiC and C/SiC mirrors for cryogenic telescope, Proc. SPIE 5494 (2004) 311–318.
[11] Hui Wang, Tingfen Cao, Zhao Xiong, Xiaodong Yuan, Chao Yao, Zheng Zhang, Guohui Ma, Optomechanical analysis of the mounting performance of large laser transport mirrors, Opt. Eng. 54 (3) (2015) 035107.
[12] Rikter Horst, Niels Tromp, Menno de Haan, Ramon Navarro, Lars Venema, Johan Pragt, Directly polished light weight aluminum mirror, Proc. SPIE 7018 (2008) 701808.
[13] Jan Kinast, Enrico Hilpert, Nicolas Lange, Andreas Gebhardt, Ralf-Rainer Rohloff, Stefan Risse, Ramona Eberhardt, Andreas Tünnermann Minimizing the bimetallic bending for cryogenic metal optics based on electroless nickel, Proc. SPIE 9151 (2014) 915136.

[14] Ziqiang Yin, Zhang Yi, Direct polishing of aluminum mirrors with higher quality and accuracy, Appl. Opt. 54 (2015) 7835–7841.
[15] Dz-Hung Gwo, Simultaneous interferometric optical-figure characteri-zations for nominal optical flat and dewar-window system at cryogenic temperatures, Proc. SPIE 2814 (1996) 36–45.
[16] David R. Hearn, Vacuum window optical power induced by temperature gradients, Proc. SPIE 3750 (1999) 297–308.